Contrasting responses of phytoplankton productivity between coastal and offshore surface waters in the Taiwan Strait and the South China Sea to short-term seawater acidification

Guang Gao[1], Tifeng Wang[1], Jiazhen Sun[1], Xin Zhao[1], Lifang Wang[1], Xianghui Guo[1], and Kunshan Gao[1,2]

[1]State Key Laboratory of Marine Environmental Science, College of Ocean and Earth Sciences,
Xiamen University, Xiamen 361005, China
[2]Co-Innovation Center of Jiangsu Marine Bio-industry Technology, Jiangsu Ocean University, Lianyungang 222005, China

Correspondence: Kunshan Gao (ksgao@xmu.edu.cn)

Abstract. Seawater acidification (SA) has been documented to either inhibit, enhance, or result in no effect on marine primary productivity (PP). In order to examine the effects of SA in changing environments, we investigated the influences of SA (a decrease of 0.4 pH_{total} units with corresponding CO_2 concentrations in the range of 22.0–39.7 µM) on PP through deck-incubation experiments at 101 stations in the Taiwan Strait and the South China Sea, including the continental shelf and slope, as well as the deepwater basin. The daily primary productivities in surface seawater under incident solar radiation ranged from 17–306 µg C $(\mu g\, Chl\, a)^{-1}\, d^{-1}$, with the responses of PP to SA being region-dependent and the SA-induced changes varying from −88 % (inhibition) to 57 % (enhancement). The SA treatment stimulated PP in surface waters of coastal, estuarine, and shelf waters but suppressed it in the South China Sea basin. Such SA-induced changes in PP were significantly related to in situ pH and solar radiation in surface seawater but negatively related to salinity changes. Our results indicate that phytoplankton cells are more vulnerable to a pH drop in oligotrophic waters. Contrasting responses of phytoplankton productivity in different areas suggest that SA impacts on marine primary productivity are region-dependent and regulated by local environments.

1 Introduction

The oceans have absorbed about one-third of anthropogenically released CO_2, which increased the dissolved CO_2 and decreased the pH of seawater (Gattuso et al., 2015), leading to ocean acidification (OA). This process is ongoing and likely intensifying (IPCC, 2019). OA has been shown to result in profound influences on marine ecosystems (see the reviews and literature in Mostofa et al., 2016, and Doney et al., 2020). Marine photosynthetic organisms, which contribute about half of the global primary production, are also being affected by OA (see the reviews and literature in Riebesell et al., 2018, and K. S. Gao et al., 2019). In addition to the slow change in ocean acidification, some processes, such as freshwater inputs, upwelling, typhoons, and eddies, can lead to instantaneous CO_2 rising and short-term changes in carbonate chemistry, termed seawater acidification (SA) (Moreau et al., 2017; Yu et al., 2020). Since SA occurs in many locations of the ocean, it is important to understand the responses of the key players of the marine biological CO_2 pump, the phytoplankton, to seawater acidification.

Elevated CO_2 is well recognized to lessen the dependence of algae and cyanobacteria on energy-consuming CO_2-concentrating mechanisms (CCMs) which concentrate CO_2 around RuBisCO, the key site for photosynthetic carbon fixation (Raven and Beardall, 2014, and references therein; Hennon et al., 2015). The energy freed up from the downregulated CCMs under increased CO_2 concentrations can be applied to other metabolic processes, resulting in a modest increase in algal growth (Wu et al., 2010; Hopkinson et al.,

2011; Xu et al., 2017). Accordingly, elevated CO_2 availability could potentially enhance marine primary productivity (Schippers et al., 2004). For instance, across 18 stations in the central Atlantic Ocean primary productivity was stimulated by 15 %–19 % under elevated dissolved CO_2 concentrations up to 36 µM (Hein and Sand-Jensen, 1997). On the other hand, the neutral effects of seawater acidification (SA) on growth rates of phytoplankton communities were reported in five of six CO_2 manipulation experiments in the coastal Pacific (Tortell et al., 2000). Furthermore, simulated future SA reduced surface PP in pelagic surface waters of the northern South China Sea and East China Sea (Gao et al., 2012). It seems that the impacts of SA on PP could be region-dependent. The varying effects of SA may be related to the regulation of other factors such as light intensity (Gao et al., 2012), temperature (Holding et al., 2015), nutrients (Tremblay et al., 2006), and community structure (Dutkiewicz et al., 2015).

The Taiwan Strait of the East China Sea, located between southeastern mainland China and the island of Taiwan, is an important channel in transporting water and biogenic elements between the East China Sea and the South China Sea. Among the Chinese coastal areas, the Taiwan Strait is distinguished by its unique location. In addition to riverine inputs, it also receives nutrients from upwelling (Hong et al., 2011). Primary productivity is much higher in coastal waters than in basin zones due to an increased supply of nutrients through river runoff and upwelling (Chen, 2003; Cloern et al., 2014). The South China Sea, located from the Equator to 23.8° N, from 99.1 to 121.1° E, and encompassing an area of about 3.5×10^6 km^2, is one of the largest marginal seas in the world. As a marginal sea of the western Pacific Ocean, it has a deep semi-closed basin (with depths > 5000 m) and wide continental shelves, characterized by a tropical and subtropical climate (Jin et al., 2016). Approximately 80 % of ocean organic carbon is buried in Earth's continental shelves, and therefore continental margins play an essential role in the ocean carbon cycle (Hedges and Keil, 1995). Investigating how SA affects primary productivity in the Taiwan Strait and the South China Sea could help us to understand the contribution of marginal seas to carbon sink under the future CO_2-increased scenarios. Although small-scale studies on SA impacts have been conducted in the East China Sea and the South China Sea (Gao et al., 2012, 2017), our understanding of how SA affects PP in marginal seas is still fragmentary and superficial. In this study, we conducted three cruises in the Taiwan Strait and the South China Sea, covering an area of 8.3×10^5 km^2, and aimed to provide in-depth insight into how SA and/or episodic pCO$_2$ rise affects PP in marginal seas with comparisons to other types of waters.

2   Materials and methods

2.1   Investigation areas

To study the impacts of projected SA (dropping by ~ 0.4 pH) by the end of this century (RCP8.5; Representative Concentration Pathway) on marine primary productivity in different areas (Gattuso et al., 2015), we carried out deck-based experiments during the three cruises supported by the National Natural Science Foundation of China (NSFC), which took place in the Taiwan Strait (14–25 July 2016), the South China Sea basin (6–24 September 2016), and the western South China Sea (14 September to 24 October 2017), respectively. The experiments were conducted at 101 stations with a coverage of 12–26° N, 110–120° E (Fig. 1). Investigation areas include the continental shelf (0–200 m, 22 stations), the slope (200–3400 m, 44 stations), and the vast deep-water basin (> 3400 m, 35 stations). In the continental shelf, the areas with depth < 50 m are defined as coastal zones (9 stations).

2.2   Measurements of temperature and carbonate chemistry parameters

The temperature and salinity of surface seawater at each station were monitored with an onboard CTD instrument (conductivity–temperature–depth; Seabird, USA). pH$_{NBS}$ was measured with an Orion 2-Star pH meter (Thermo Scientific, USA) that was calibrated with standard National Bureau of Standards (NBS) buffers (pH = 4.01, 7.00, and 10.01 at 25.0 °C; Thermo Fisher Scientific Inc., USA). After the calibration, the electrode of the pH meter was kept in surface seawater for half an hour, and then the formal measurements were conducted. The analytical precision was ±0.001. Total alkalinity (TA) was determined using Gran titration on a 25 mL sample with a TA analyser (AS-ALK1, Apollo SciTech, USA) that was regularly calibrated with certified reference materials supplied by Andrew G. Dickson at the Scripps Institution of Oceanography (Gao et al., 2018a). The analytical precision was ±2 µmol kg^{-1}. CO_2 concentration in seawater and the pH$_{Total}$ (pH$_T$) values were calculated by using CO2SYS (Pierrot et al., 2006) with the input of pH$_{NBS}$ and TA data.

2.3   Solar radiation

The incident solar radiation intensity during the cruises was recorded with an Eldonet broadband filter radiometer (Eldonet XP, Real Time Computer, Germany). This device has three channels for PAR (photosynthetically active radiation; 400–700 nm), UV-A (315–400 nm), and UV-B (280–315 nm) irradiance, respectively, for recording the means of solar radiations each minute. The instrument was fixed at the top layer of the ship to avoid shading.
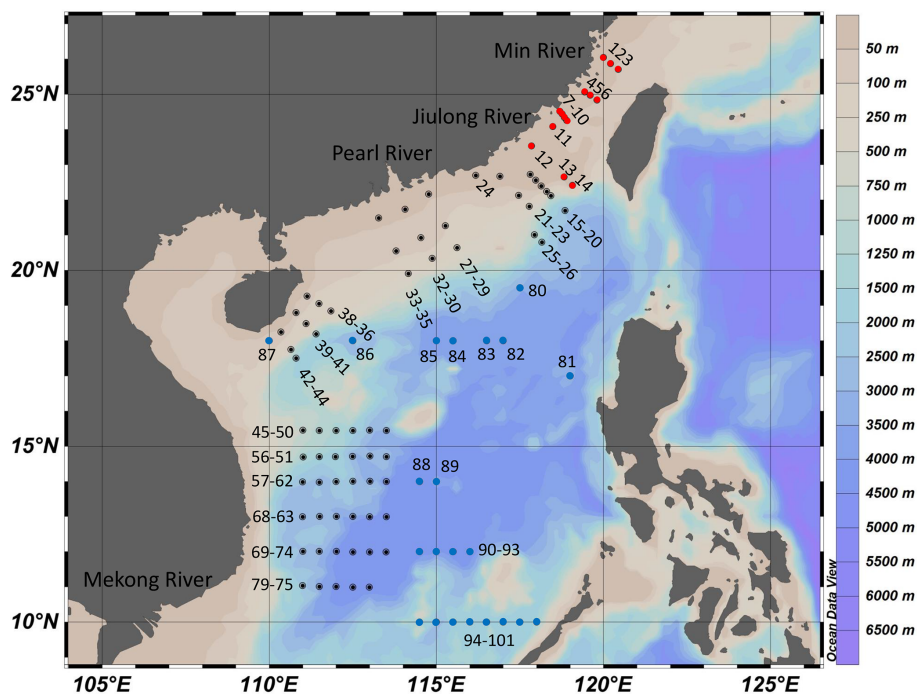
Figure 1. Sampling stations for the incubation experiments in the Taiwan Strait and the South China Sea during three cruises. The Taiwan Strait cruise was conducted in July 2016 (red dots); the South China Sea basin cruise was conducted in September 2016 (blue dots); and the western South China Sea cruise was conducted in September 2017 (black dots).

2.4 Determination of primary productivity

Surface seawater (0–1 m) was collected with a 10 L acid-cleaned (1 M HCl) plastic bucket and pre-filtered (200 μm mesh size) to remove large grazers. To prepare high-CO_2 (HC) seawater, CO_2-saturated seawater was added into pre-filtered seawater until a decrease of ∼ 0.4 units of pH (corresponding CO_2 concentrations being 22.0–39.7 μM) was approached (Gattuso et al., 2010). Seawater that was collected from the same location as PP and filtered by cellulose acetate membrane (0.22 μm) was used to make the CO_2-saturated seawater, which was made by directly flushing with pure CO_2 until pH reached values around 4.50. When CO_2-saturated seawater was added to the HC treatment, equivalent filtered seawater (without flushing with CO_2) was also added to the ambient-CO_2 (AC) treatment as a control. The ratios of added CO_2-saturated seawater to incubation seawater were about 1 : 1000. Samples were incubated within half an hour after they were collected. Prepared AC and HC seawater was allocated into 50 mL quartz tubes in triplicate, inoculated with 5 μCi (curie) (0.185 MBq) $NaH^{14}CO_3$ (ICN Radiochemicals, USA), and then incubated for 24 h (over a day–night cycle) under 100 % incident solar irradiances in a water bath for temperature control by running it through surface seawater. Due to heating by the deck, the temperatures in the water bath were 0–2 °C higher than in situ surface seawater temperatures. The TA and pH values of seawater before and after 24 h incubation were measured to moni-

tor the changes in carbonate systems. After the incubation, the cells were filtered onto glass microfibre filters (GF/F, Whatman) and immediately frozen at −20 °C for later analysis. In the laboratory, the frozen filters were transferred to 20 mL scintillation vials, thawed and exposed to HCl fumes for 12 h, and dried (55 °C, 6 h) to expel non-fixed ^{14}C, as previously reported (Gao et al., 2017). Then a 3 mL scintillation cocktail (PerkinElmer®, OptiPhase HiSafe) was added to each vial. After 2 h of reaction, the incorporated radioactivity was counted by liquid scintillation counting (LS 6500, Beckman Coulter, USA). The carbon fixation for 24 h incubation was taken as chlorophyll a-normalized (Chl a) daily primary productivity (PP, μg C (μg Chl a)$^{-1}$) (Gao et al., 2017). The changes (%) in PP induced by SA were expressed as $(PP_{HC} - PP_{AC})/PP_{AC} \times 100$, where PP_{HC} and PP_{AC} are the daily primary productivity under HC and AC, respectively.

2.5 Chl a measurement

Pre-filtered (200 μm mesh size) surface seawater (500–2000 mL) at each station was filtered onto a GF/F filter (25 mm, Whatman) and then stored at −80 °C. After returning to laboratory, phytoplankton cells on the GF/F filter were extracted overnight in absolute methanol at 4 °C in darkness. After centrifugation (5000 g for 10 min), the absorption values of the supernatants were analysed by a UV–Vis spectrophotometer (DU800, Beckman, Fullerton, California,

USA). The concentration of chlorophyll a (Chl a) was calculated according to Porra (2002).

2.6 Data analysis

The data of environmental parameters were expressed in raw values, and the data of PP were the means of triplicate incubations. Two-way analysis of variance (ANOVA) was used to analyse the effects of SA and location on PP. Least significant difference (LSD) was used to for post hoc analysis. Linear fitting analysis was conducted with Pearson correlation analysis to assess the relationship between PP and environmental factors. A 95 % confidence level was used in all analyses.

3 Results

During the cruises, surface temperature ranged from 25.0 to 29.9 °C in the Taiwan Strait and from 27.1 to 30.2 °C in the South China Sea (Fig. 2a). Surface salinity ranged from 30.0 to 34.0 in the Taiwan Strait and from 31.0 to 34.3 in the South China Sea (Fig. 2b). The lower salinities were found in the estuaries of the Min River and Jiulong River as well as the Mekong River-induced rip current. High salinities were found in the South China Sea basin. Surface pH_T changed between 7.99–8.20 in the Taiwan Strait, with the higher values in the estuary of Min River (Fig. 2c). Compared to the Taiwan Strait, the South China Sea had lower surface pH (7.91–8.08), with the lowest value near an island in the Philippines. TA ranged from 2100 to 2359 $\mu mol\,kg^{-1}$ SW in the Taiwan Strait and 2126 to 2369 $\mu mol\,kg^{-1}$ SW in the South China Sea (Fig. 2d). The lowest value occurred in the estuary of Min River. CO_2 concentration in surface seawater changed from 6.4–13.3 $\mu mol\,kg^{-1}$ SW in the Taiwan Strait and 9.3–14.3 $\mu mol\,kg^{-1}$ SW in the South China Sea (Fig. 2e). It showed an opposite pattern to surface pH, with the lowest value in the estuary of the Min River in the Taiwan Strait and the highest value in the South China Sea near islands in the Philippines. During the PP investigation period, the daytime mean PAR intensity ranged from 126.6 to 145.2 $W\,m^{-2}$ in the Taiwan Strait and 37.3 to 150.0 $W\,m^{-2}$ in the South China Sea (Fig. 2f).

The concentration of Chl a ranged from 0.11 to 12.13 $\mu g\,L^{-1}$ in the Taiwan Strait (Fig. 3). The highest concentration occurred in the estuary of the Min River. The concentration of Chl a in the South China Sea ranged from 0.037 to 7.43 $\mu g\,L^{-1}$. The highest concentration was found in the coastal areas of the province of Guangdong in China. For both the Taiwan Strait and the South China Sea, there were high Chl a concentrations ($> 1.0\,\mu g\,L^{-1}$) in coastal areas, particularly in the estuaries of the Min River, Jiulong River, and Pearl River. On the contrary, Chl a concentrations in offshore areas were lower than 0.2 $\mu g\,L^{-1}$.

Surface primary productivity changed from 99 to 302 $\mu g\,C\,(\mu g\,Chl\ a)^{-1}\,d^{-1}$ in the Taiwan Strait and from 17 to 306 $\mu g\,C\,(\mu g\,Chl\ a)^{-1}\,d^{-1}$ in the South China Sea (Fig. 4). High surface primary productivity ($> 200\,\mu g\,C\,(\mu g\,Chl\ a)^{-1}\,d^{-1}$) was found in the estuaries of the Min River, Jiulong River, and Pearl River and areas near the east of Vietnam. In basin zones, the surface primary productivity was usually lower than 100 $\mu g\,C\,(\mu g\,Chl\ a)^{-1}\,d^{-1}$.

A series of onboard CO_2-enriched experiments in the investigated regions were conducted during the three cruises. In HC treatments, pH_{total} decreased by 0.34–0.43 units, while pCO_2 and CO_2 increased by 676–982 μatm and 17–25 $\mu mol\,kg^{-1}$ SW, respectively (Table S1 in the Supplement). Carbonate chemistry parameters after 24 h of incubation were stable (pH < 0.06, TA < 53 $\mu mol\,kg^{-1}$ SW), indicating the successful manipulation (Table S1). It was observed that instantaneous effects of elevated pCO_2 on primary productivity of the surface phytoplankton community in all investigated regions ranged from −88 % (inhibition) to 57 % (promotion), revealing significant regional differences among the continental shelf, slope, and deep-water basin (ANOVA, $F_{(2,98)} = 3.747$, $p = 0.027$, Fig. 5). Among 101 stations, 70 stations showed insignificant SA effects. SA increased PP at 6 stations and reduced PP at 25 stations. Positive effects of SA on surface primary productivity were observed in the Taiwan Strait and the western South China Sea (Fig. 5, areas with red–yellow shading), with the maximal enhancement of 57 % in the station approaching the Mekong River plume (LSD, $p < 0.001$). Reductions in PP induced by the elevated CO_2 were mainly found in the central South China Sea basin within 10–14° N, 114.5–118° E (Fig. 5, areas with blue–purple shading), with inhibition rates ranging from 24 % to 88 % (Fig. 5, LSD, $p < 0.05$). These results showed a region-related effect of SA on photosynthetic carbon fixation of surface phytoplankton assemblages. Overall, the elevated pCO_2 had neutral or positive effects on primary productivity in the continental shelf and slope regions, while it had adverse effects in the deep-water basin.

By analysing the correlations between SA-induced PP changes and regional environmental parameters (Table S2), we found that SA-induced changes in phytoplankton primary productivity was significantly positively related to in situ pH ($p < 0.001$, $r = 0.379$) and PAR density ($p = 0.002$, $r = 0.311$) (Fig. 6). On the other hand, the influence induced by SA was negatively related to salinity, which ranged from 30.00 to 34.28 ($p < 0.001$, $r = -0.418$).

4 Discussion

In the present study, we found that the elevated pCO_2 and associated pH drop increased or did not affect PP in the continental shelf and slope waters but reduced it in basin waters. Our results suggested that the enhanced effects of
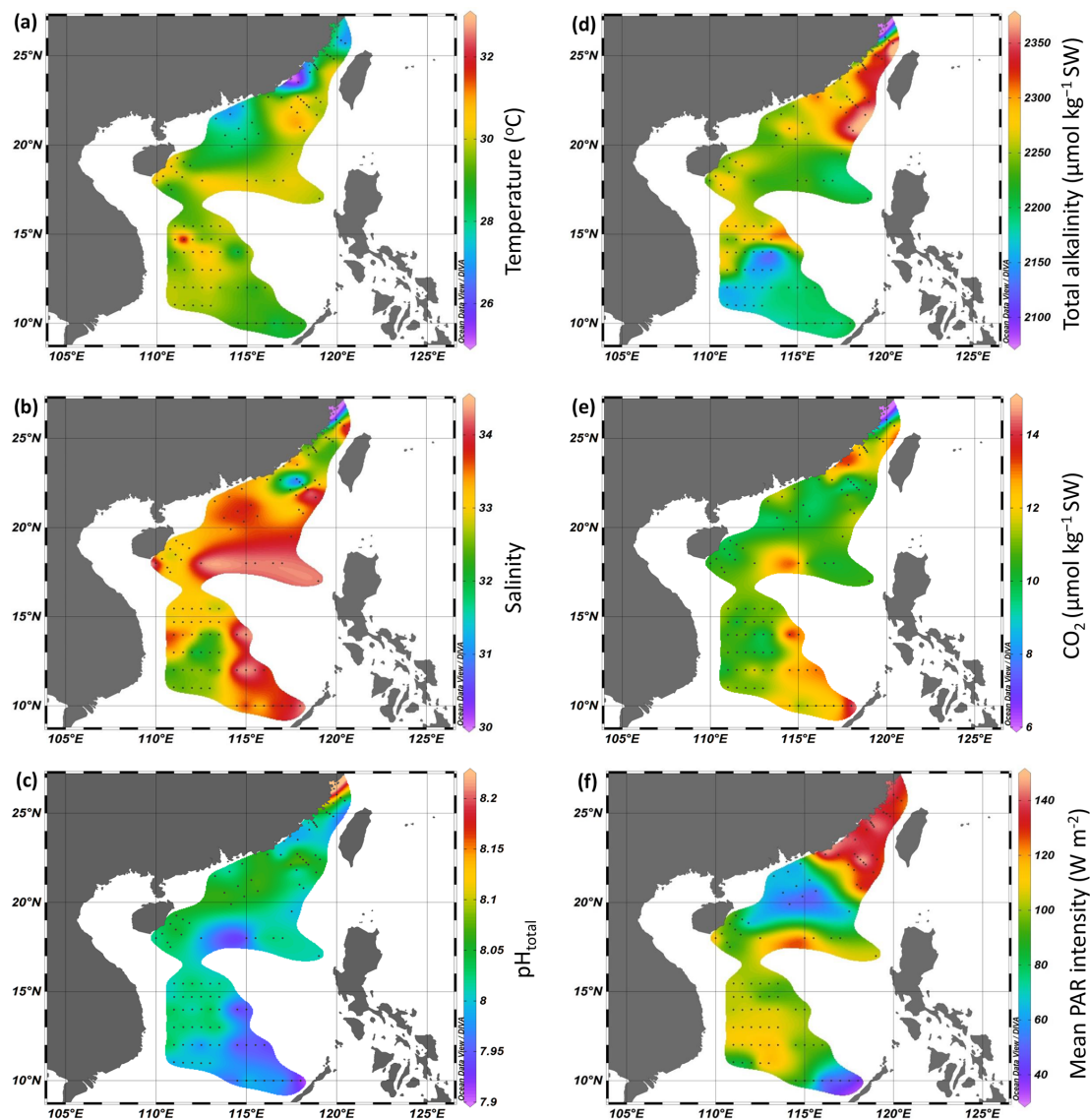
Figure 2. Temperature (°C, **a**), salinity (**b**), pH_{total} (**c**), total alkalinity ($\mu mol\,kg^{-1}$ SW, **d**), and CO_2 ($\mu mol\,kg^{-1}$ SW, **e**) in surface seawater (SW) and mean PAR intensity (W m^{-2}, **f**) during the PP incubation experiments.

the SA treatment on photosynthetic carbon fixation depend on regions of different physicochemical conditions, including pH, light intensity, and salinity. In addition, coastal diatoms appear to benefit more from SA than pelagic ones (Li et al., 2016). Therefore, community structure differences might also be responsible for the contrasts of the short-term high-CO_2-induced acidification between coastal and basin waters.

SA is deemed to have two kinds of effects at least (Xu et al., 2017; Shi et al., 2019). The first one is the enrichment of CO_2, which is usually beneficial for photosynthetic carbon fixation and the growth of algae because insufficient ambient CO_2 limits algal photosynthesis (Hein and Sand-Jensen, 1997; Bach and Taucher, 2019). The other effect is

the decreased pH which could be harmful because it disturbs the acid–base balance between extracellular and intracellular environments. For instance, the decreased pH projected for future SA was shown to reduce the growth of the diazotroph *Trichodesmium* (Hong et al., 2017), decrease PSII (photosystem II) activity by reducing the removal rate of PsbD (D2) (Gao et al., 2018b), and increase mitochondrial and photo-respirations in diatoms and phytoplankton assemblages (Yang and Gao, 2012; Jin et al., 2015). In addition, SA could reduce the RuBisCO transcription of diatoms, which also contributed to the decreased growth (Endo et al., 2015). Therefore, the net impact of SA depends on the balance between its positive and negative effects, leading to enhanced, inhibited, or neutral influences, as reported in di-
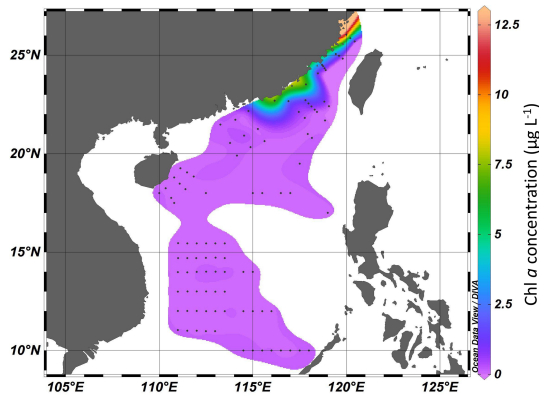
Figure 3. Chl a concentration (μg L^{-1}) in the Taiwan Strait and the South China Sea during research cruises.
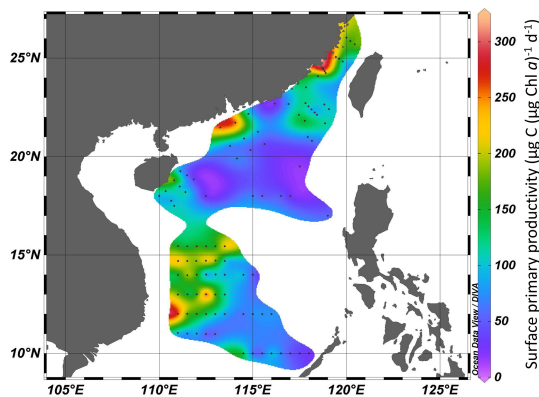

Figure 4. Surface primary productivity (μg C (μg Chl a)$^{-1}$ d^{-1}) in the Taiwan Strait and the South China Sea during research cruises.

Figure 5. Seawater-acidification-induced (pH decreases of 0.4 units) changes (%) of surface primary productivity in the Taiwan Strait and the South China Sea. Red–yellow shading represents a positive effect on PP, and blue–purple shading represents a negative effect.

Figure 6. Seawater-acidification-induced (pH decreases of 0.4 units) changes on surface primary productivity (%) in the Taiwan Strait and the South China Sea as a function of ambient pH$_{total}$ **(a)**, PAR **(b)**, and salinity **(c)**. The dotted lines represent 95 % confidence intervals.

atoms (Gao et al., 2012; Li et al., 2021) and phytoplankton assemblages in the Arctic and sub-Arctic shelf seas (Hoppe et al., 2018), the North Sea (Eberlein et al., 2017), and the South China Sea (Gao et al., 2012). The balance of positive and negative effects of SA can be regulated by other factors, including pH, light intensity, salinity, and population structure, among others (K. S. Gao et al., 2019; G. Gao et al., 2019; Xie et al., 2022).

In the present study, SA increased or did not affect PP in coastal waters but reduced it in offshore waters, which is significantly related to pH, light intensity, and salinity (Fig. 6). The effect of SA changed from negative to positive with the increase in local pH. The higher pH occurred in coastal zones which may be caused by the higher biomass of phytoplankton (Fig. 3). Higher pH caused by intensive photosynthesis of phytoplankton is companied with decreased CO$_2$ levels. In this case, CO$_2$ is more limiting for the photosynthesis of phytoplankton compared to lower pH. Therefore, SA could stimulate primary productivity via supplying more available CO$_2$ (Hurd et al., 2019). On the other hand, lower pH occurred in the deep-water basin. Lower pH represents higher
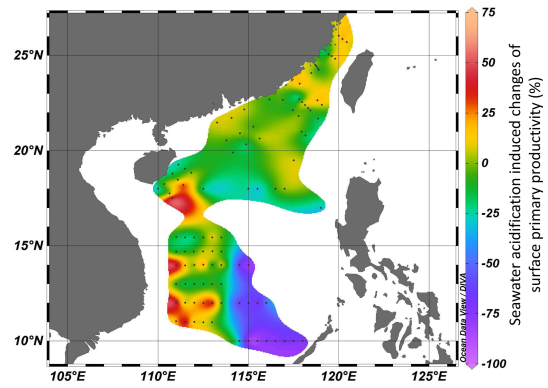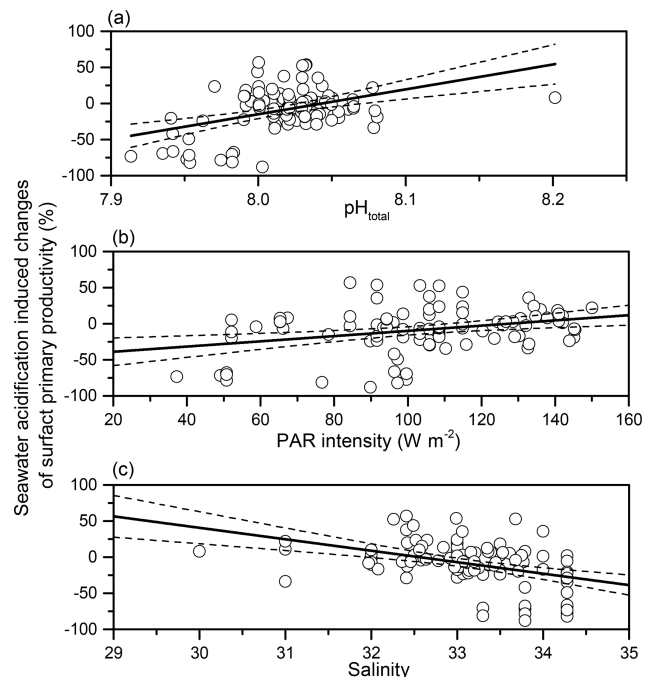
CO$_2$ availability. CO$_2$ is not limited or less limited in this case. Therefore, more CO$_2$ brought by SA may not benefit the photosynthesis of phytoplankton. Instead, decreased pH accompanied by SA may inhibit the photosynthesis or growth of phytoplankton, which is found in cyanobacteria (Hong et al., 2017). Furthermore, the negative effects of SA are particularly significant when nutrients are limited (Li et al., 2018). The nutrient levels in the basin are usually lower

than on the shelf (Yuan et al., 2011; Lu et al., 2020; Du et al., 2021), which may exacerbate the negative effects of SA in the basin zone.

The negative effects of SA disappeared with increasing light intensity in this study. This results in inconsistency with the study of Gao et al. (2012), in which SA increased photosynthetic carbon fixation of three diatoms (*Phaeodactylum tricornutum*, *Thalassiosira pseudonana*, and *Skeletonema costatum*) under lower light intensities but decreased it under higher light intensities. The divergent findings may be due to a different population structure that varies in different areas. Coastal zones where nutrients are relatively sufficient usually have abundant diatoms, while picophytoplankton, mainly *Prochlorococcus* and *Synechococcus*, dominate oligotrophic areas (Xiao et al., 2018; Zhong et al., 2020). In this study, most investigated areas are oligotrophic, and thus the response of local phytoplankton to the combination of light intensity and SA may be different from diatoms. Meanwhile, the weak correlation ($r = 0.311$) between light intensity and SA effect suggests the deviation from the linear relationship in the context of multiple variables needs to be further illuminated in future studies. It is worth noting that the samples were not mixed down in the water bath in the present study and exposed to 100 % incident solar irradiances. Lower incident solar irradiances or some devices can be used to simulate seawater mixing in future studies. A negative correlation between SA-induced changes in PP and salinity was found in this study. The decrease in salinity (from 35 to 30) has been shown to alleviate the negative effect of SA on the photosynthetic carbon fixation of the coccolithophorid *Emiliania huxleyi* (Xu et al., 2020), although the potential mechanisms remain unknown. On the other hand, the change in salinity (from 6 to 3) did not affect the effective quantum yield of the microplanktonic community in the Baltic Sea grown under different CO_2 levels (Wulff et al., 2018). In this study, the negative relationship between salinity and SA effects seems to be an autocorrelation between salinity and in situ pH (Fig. S1 in the Supplement) because lower salinity occurred in coastal waters where seawater pH was higher, while the basin zone usually had higher salinities and lower pH.

The specific environmental conditions have profound effects on shaping diverse dominant phytoplankton groups (Boyd et al., 2010). Larger eukaryotic groups (especially diatoms) usually dominate the complex coastal regions, while picophytoplankton (*Prochlorococcus* and *Synechococcus*), characterized by more efficient nutrient uptake, dominate the relatively stable offshore waters (Dutkiewicz et al., 2015). In summer and early autumn, previous investigations demonstrated that diatoms dominated in the northern waters and the Taiwan Strait (coastal and shelf regions) with high abundances of phytoplankton, which is consistent with our Chl *a* data; *Prochlorococcus* and *Synechococcus* dominated in the South China Sea basin and the north of the South China Sea (slope and basin regions) (Xiao et al., 2018; Zhong et al.,

2020). In addition, it has been reported that larger cells benefit more from SA because a thicker diffusion layer around the cells limits the transport of CO_2 (Feng et al., 2010; Wu et al., 2014). In contrast, a thinner diffusion layer and higher surface-to-volume ratio in smaller phytoplankton cells can make transporting CO_2 near the cell surface and within the cells easier, and therefore picophytoplankton species are less CO_2-limited (Bao and Gao, 2021). Therefore, different community structures between coastal and basin areas could also be responsible for the enhanced and inhibitory effects of SA. It is worth noting that seasonality may also lead to the differential effects of SA on primary productivity, since the Taiwan Strait cruise was conducted in July, whereas the cruises of the South China Sea basin and the western South China Sea were conducted in September. The seas surface temperature (SST) and solar PAR intensity of the Taiwan Strait in July were 2–3 °C and 22 ± 22 W m^{-2} higher than in September (Zhang et al., 2008, 2009; Table S3). Although the effects of SA were not related to temperature as shown in this study (Table S2), the higher solar radiation in July may contribute to the positive effect of SA on primary productivity. In addition, seasonal phytoplankton species succession may also affect the response to SA (Xiao et al., 2018).

5   Conclusions

By investigating the impacts of the elevated $p\mathrm{CO_2}$ on PP in the Taiwan Strait and the South China Sea, we demonstrated that such short SA-treatment-induced changes in PP were mainly related to pH, light intensity, and salinity based on Pearson correlation coefficients, supporting the hypothesis that negative impacts of SA on PP increase from coastal to basin waters (K. S. Gao et al., 2019). In addition, changes in phytoplankton community structure may also modulate the SA-induced variability. In view of ocean climate changes, strengthened stratification due to global warming would reduce the upward transport of nutrients and thus marine primary productivity. The negative effect of SA in basin zones may further reduce primary productivity. Meanwhile, PP in some coastal waters may be increased by SA.

References

Bach, L. T. and Taucher, J.: CO_2 effects on diatoms: a synthesis of more than a decade of ocean acidification experiments with natural communities, Ocean Sci., 15, 1159–1175, https://doi.org/10.5194/os-15-1159-2019, 2019.

Bao, N. and Gao, K.: Interactive effects of elevated CO_2 concentration and light on the picophytoplankton *Synechococcus*, Front. Mar. Sci., 8, 1–7, 2021.

Boyd, P. W., Strzepek, R., Fu, F. X., and Hutchins, D. A.: Environmental control of open-ocean phytoplankton groups: Now and in the future, Limnol. Oceanogr., 55, 1353–1376, 2010.

Chen, C. T. A.: Rare northward flow in the Taiwan Strait in winter: A note, Cont. Shelf Res., 23, 387–391, 2003.

Cloern, J. E., Foster, S. Q., and Kleckner, A. E.: Phytoplankton primary production in the world's estuarine-coastal ecosystems, Biogeosciences, 11, 2477–2501, https://doi.org/10.5194/bg-11-2477-2014, 2014.

Doney, S. C., Busch, D. S., Cooley, S. R., and Kroeker, K. J.: The impacts of ocean acidification on marine ec–systems and reliant human communities, Annu. Rev. Environ. Resour., 45, 83-112, 2020.

Du, C., He, R., Liu, Z., Huang, T., Wang, L., Yuan, Z., Xu, Y., Wang, Z., and Dai, M.: Climatology of nutrient distributions in the South China Sea based on a large data set derived from a new algorithm, Prog. Oceanogr., 195, 102586, https://doi.org/10.1016/j.pocean.2021.102586, 2021.

Dutkiewicz, S., Morris, J. J., Follows, M. J., Scott, J., Levitan, O., Dyhrman, S. T., and Berman-Frank, I.: Impact of ocean acidification on the structure of future phytoplankton communities, Nat. Clim. Change, 5, 1002–1006, 2015.

Eberlein, T., Wohlrab, S., Rost, B., John, U., Bach, L. T., Riebesell, U., and Van de Waal, D. B.: Effects of ocean acidification on primary production in a coastal North Sea phytoplankton community, Plos One, 12, 1–15, 2017.

Endo, H., Sugie, K., Yoshimura, T., and Suzuki, K.: Effects of CO_2 and iron availability on rbcL gene expression in Bering Sea diatoms, Biogeosciences, 12, 2247–2259, https://doi.org/10.5194/bg-12-2247-2015, 2015.

Feng, Y., Hare, C. E., Rose, J. M., Handy, S. M., DiTullio, G. R., Lee, P. A., Smith, W. O., Peloquin, J., Tozzi, S., Sun, J., Zhang, Y., Dunbar, R. B., Long, M. C., Sohst, B., Lohan, M., and Hutchins, D. A.: Interactive effects of iron, irradiance and CO_2 on Ross Sea phytoplankton, Deep-Sea Res. Pt. I, 57, 368–383, 2010.

Gao, G., Jin, P., Liu, N., Li, F. T., Tong, S. Y., Hutchins, D. A., and Gao, K. S.: The acclimation process of phytoplankton biomass, carbon fixation and respiration to the combined effects of elevated temperature and $p\mathrm{CO}_2$ in the northern South China Sea, Mar. Pollut. Bull., 118, 213–220, 2017.

Gao, G., Xia, J., Yu, J., Fan, J., and Zeng, X.: Regulation of inorganic carbon acquisition in a red tide alga (*Skeletonema costatum*): the importance of phosphorus availability, Biogeosciences, 15, 4871–4882, https://doi.org/10.5194/bg-15-4871-2018, 2018a.

Gao, G., Xu, Z. G., Shi, Q., and Wu, H. Y.: Increased CO_2 exacerbates the stress of ultraviolet radiation on photosystem II function in the diatom *Thalassiosira weissflogii*, Environ. Exp. Bot., 156, 96–105, 2018b.

Gao, G., Qu, L., Xu, T., Burgess, J. G., Li, X., and Xu, J.: Future CO_2-induced ocean acidification enhances resilience of a green tide alga to low-salinity stress, ICES J. Mar. Sci., 76, 2437–2445, 2019.

Gao, K. S., Xu, J. T., Gao, G., Li, Y. H., Hutchins, D. A., Huang, B. Q., Wang, L., Zheng, Y., Jin, P., Cai, X. N., Hader, D. P., Li, W., Xu, K., Liu, N. N., and Riebesell, U.: Rising CO_2 and increased light exposure synergistically reduce marine primary productivity, Nat. Clim. Change, 2, 519–523, 2012.

Gao, K. S., Beardall, J., Häder, D. P., Hall-Spencer, J. M., Gao, G., and Hutchins, D. A.: Effects of ocean acidification on marine photosynthetic organisms under the concurrent influences of warming, UV radiation, and deoxygenation, Front. Mar. Sci., 6, 1–18, 2019.

Gattuso, J. P., Gao, K. S., Lee, K., Rost, B., and Schulz, K. G.: Approaches and tools to manipulate the carbonate chemistry, in: Guide to best practices for ocean acidification research and data reporting, edited by: Riebesell, U., Fabry, V. J., Hansson, L., and Gattuso, J.-P., Publications Office of the European Union, Luxembourg, 41–52, https://oceanrep.geomar.de/id/eprint/10310 (last access: 28 May 2022), 2010.

Gattuso, J. P., Magnan, A., Billé, R., Cheung, W. W. L., Howes, E. L., Joos, F., Allemand, D., Bopp, L., Cooley, S. R., Eakin, C. M., Hoegh-Guldberg, O., Kelly, R. P., Portner, H. O., Rogers, A. D., Baxter, J. M., Laffoley, D., Osborn, D., Rankovic, A., Rochette, J., Sumaila, U. R., Treyer, S., and Turley, C.: Contrasting futures for ocean and society from different anthropogenic CO_2 emissions scenarios, Science, 349, aac4722, https://doi.org/10.1126/science.aac472, 2015.

Hedges, J. I., and Keil, R. G.: Sedimentary organic matter preservation: an assessment and speculative synthesis, Mar. Chem., 49, 81–115, 1995.

Hein, M., and Sand-Jensen, K.: CO_2 increases oceanic primary production, Nature, 388, 526–527, 1997.

Hennon, G. M. M., Ashworth, J., Groussman, R. D., Berthiaume, C., Morales, R. L., Baliga, N. S., Orellana, M. V., and Armbrust, E. V.: Diatom acclimation to elevated CO_2 via cAMP signalling and coordinated gene expression, Nat. Clim. Change, 5, 761–765, 2015.

Holding, J. M., Duarte, C. M., Sanz-Martín, M., Mesa, E., Arrieta, J. M., Chierici, M., Hendriks, I. E., Garcia-Corral, L. S., Regaudie-de-Gioux, A., Delgado, A., Reigstad, M., Wassmann, P., and Agusti, S.: Temperature dependence of CO_2-enhanced primary production in the European Arctic Ocean, Nat. Clim. Change, 5, 1079–1082, 2015.

Hong, H. S., Chai, F., Zhang, C. Y., Huang, B. Q., Jiang, Y. W., and Hu, J. Y.: An overview of physical and biogeochemical processes and ecosystem dynamics in the Taiwan Strait, Cont. Shelf Res., 31, S3–S12, 2011.

Hong, H. Z., Shen, R., Zhang, F. T., Wen, Z. Z., Chang, S. W., Lin, W. F., Kranz, S. A., Luo, Y. W., Kao, S. J., Morel, F. M. M., and Shi, D. L.: The complex effects of ocean acidification on the prominent N_2-fixing cyanobacterium *Trichodesmium*, Science, 356, 527–530, 2017.

Hopkinson, B. M., Dupont, C. L., Allen, A. E., and Morel, F. M.: Efficiency of the CO_2-concentrating mechanism of diatoms, P. Natl. Acad. Sci. USA., 108, 3830–3837, 2011.

Hoppe, C. J. M., Wolf, K. K. E., Schuback, N., Tortell, P. D., and Rost, B.: Compensation of ocean acidification effects in Arctic phytoplankton assemblages, Nat. Clim. Change, 8, 529–533, 2018.

Hurd, C. L., Beardall, J., Comeau, S., Cornwall, C. E., Havenhand, J. N., Munday, P. L., Parker, L. M., Raven, J. A., and McGraw, C. M.: Ocean acidification as a multiple driver: how interactions between changing seawater carbonate parameters affect marine life, Mar. Freshwater Res., 71, 263–274, 2019.

IPCC: IPCC Special Report on the Ocean and Cryosphere in a Changing Climate, edited by: Pörtner, H.-O., Roberts, D. C., Masson-Delmotte, V., Zhai, P., Tignor, M., Poloczanska, E., Mintenbeck, K., Alegría, A., Nicolai, M., Okem, A., Petzold, J., Rama, B., and Weyer, N. M., Cambridge University Press, Cambridge, UK and New York, NY, USA, 755 pp., https://doi.org/10.1017/9781009157964, 2019.

Jin, P., Wang, T. F., Liu, N. N., Dupont, S., Beardall, J., Boyd, P. W., Riebesell, U., and Gao, K. S.: Ocean acidification increases the accumulation of toxic phenolic compounds across trophic levels, Nat. Commun., 6, 1–6, 2015.

Jin, P., Gao, G., Liu, X., Li, F. T., Tong, S. Y., Ding, J. C., Zhong, Z. H., Liu, N. N., and Gao, K. S.: Contrasting photophysiological characteristics of phytoplankton assemblages in the Northern South China Sea, Plos One, 11, 1–16, 2016.

Li, F., Wu, Y., Hutchins, D. A., Fu, F., and Gao, K.: Physiological responses of coastal and oceanic diatoms to diurnal fluctuations in seawater carbonate chemistry under two CO_2 concentrations, Biogeosciences, 13, 6247–6259, https://doi.org/10.5194/bg-13-6247-2016, 2016.

Li, F. T., Beardall, J., and Gao, K. S.: Diatom performance in a future ocean: interactions between nitrogen limitation, temperature, and CO_2-induced seawater acidification, ICES J. Mar. Sci., 75, 1451–1464, 2018.

Li, H., Xu, T., Ma, J., Li, F., and Xu, J.: Physiological responses of *Skeletonema costatum* to the interactions of seawater acidification and the combination of photoperiod and temperature, Biogeosciences, 18, 1439–1449, https://doi.org/10.5194/bg-18-1439-2021, 2021.

Lu, Z., Gan, J., Dai, M., Zhao, X., and Hui, C. R.: Nutrient transport and dynamics in the South China Sea: A modeling study, Prog. Oceanogr., 183, 102308, https://doi.org/10.1016/j.pocean.2020.102308, 2020.

Moreau, S., Penna, A. D., Llort, J., Patel, R., Langlais, C., Boyd, P. W., Matear, R. J., Phillips, H. E., Trull, T. W., Tilbrook, B., and Lenton, A.: Eddy-induced carbon transport across the Antarctic Circumpolar Current, Global Biogeochem. Cy., 31, 1368–1386, 2017

Mostofa, K. M. G., Liu, C.-Q., Zhai, W., Minella, M., Vione, D., Gao, K., Minakata, D., Arakaki, T., Yoshioka, T., Hayakawa, K., Konohira, E., Tanoue, E., Akhand, A., Chanda, A., Wang, B., and Sakugawa, H.: Reviews and Syntheses: Ocean acidification and its potential impacts on marine ecosystems, Biogeosciences, 13, 1767–1786, https://doi.org/10.5194/bg-13-1767-2016, 2016.

Pierrot, D., Wallace, D. W. R., and Lewis, E.: MS Excel program developed for CO_2 system calculations, ORNL/CDIAC-105a, Carbon Dioxide Information Analysis Center, Oak Ridge National Laboratory, US Department of Energy, Oak Ridge, Tennessee, USA, https://doi.org/10.3334/CDIAC/otg.CO2SYS_XLS_CDIAC105a, 2006.

Porra, R. J.: The chequered history of the development and use of simultaneous equations for the accurate determination of chlorophylls *a* and *b*, Photosynth. Res., 73, 149–156, 2002.

Raven, J. A. and Beardall, J.: CO_2 concentrating mechanisms and environmental change, Aquat. Bot., 118, 24–37, 2014.

Riebesell, U., Aberle-Malzahn, N., Achterberg, E. P., Algueró-Muñiz, M., Alvarez-Fernandez, S., Arístegui, J., Bach, L. T., Boersma, M., Boxhammer, T., Guan, W. C., Haunost, M., Horn, H. G., Loscher, C. R., Ludwig, A., Spisla, C., Sswat, M., Stange, P., and Taucher, J.: Toxic algal bloom induced by ocean acidification disrupts the pelagic food web, Nat. Clim. Change, 8, 1082–1086, 2018.

Schippers, P., Lürling, M., and Scheffer, M.: Increase of atmospheric CO_2 promotes phytoplankton productivity, Ecol. Lett., 7, 446–451, 2004.

Shi, D. L., Hong, H. Z., Su, X., Liao, L. R., Chang, S. W., and Lin, W. F.: The physiological response of marine diatoms to ocean acidification: Differential roles of seawater pCO_2 and pH, J. Phycol., 55, 521–533, 2019.

Tortell, P. D., Rau, G. H., and Morel, F. M. M.: Inorganic carbon acquisition in coastal Pacific phytoplankton communities, Limnol. Oceanogr., 45, 1485–1500, 2000.

Tremblay, J. E., Michel, C., Hobson, K. A., Gosselin, M., and Price, N. M.: Bloom dynamics in early opening waters of the Arctic Ocean, Limnol. Oceanogr., 51, 900–912, 2006.

Wu, Y., Gao, K., and Riebesell, U.: CO_2-induced seawater acidification affects physiological performance of the marine diatom *Phaeodactylum tricornutum*, Biogeosciences, 7, 2915–2923, https://doi.org/10.5194/bg-7-2915-2010, 2010.

Wu, Y., Campbell, D. A., Irwin, A. J., Suggett, D. J., and Finkel, Z. V.: Ocean acidification enhances the growth rate of larger diatoms, Limnol. Oceanogr., 59, 1027–1034, 2014.

Wulff, A., Karlberg, M., Olofsson, M., Torstensson, A., Riemann, L., Steinhoff, F. S., Mohlin, M., Ekstrand, N., and Chierici, M.: Ocean acidification and desalination: Climate-driven change in a Baltic Sea summer microplanktonic community, Mar. Biol., 165, 1–15, 2018.

Xiao, W. P., Wang, L., Laws, E., Xie, Y. Y., Chen, J. X., Liu, X., Chen, B. Z., and Huang, B. Q.: Realized niches explain spatial gradients in seasonal abundance of phytoplankton groups in the South China Sea, Prog. Oceanogr., 162, 223–239, 2018.

Xie, S., Lin, F., Zhao, X., and Gao, G.: Enhanced lipid productivity coupled with carbon and nitrogen removal of the diatom *Skeletonema costatum* cultured in the high CO_2 level, Algal. Res., 61, 102589, https://doi.org/10.1016/j.algal.2021.102589, 2022.

Xu, J. K., Sun, J. Z., Beardall, J., and Gao, K. S.: Lower salinity leads to improved physiological performance in the coccolithophorid *Emiliania huxleyi*, which partly ameliorates the effects of ocean acidification, Front. Mar. Sci., 7, 1–18, 2020.

Xu, Z., Gao, G., Xu, J., and Wu, H.: Physiological response of a golden tide alga (*Sargassum muticum*) to the interaction of ocean acidification and phosphorus enrichment, Biogeosciences, 14, 671–681, https://doi.org/10.5194/bg-14-671-2017, 2017.

Yang, G. Y. and Gao, K. S.: Physiological responses of the marine diatom *Thalassiosira pseudonana* to increased pCO_2 and seawater acidity, Mar. Environ. Res., 79, 142–151, 2012.

Yu, P., Wang, Z. A., Churchill, J., Zheng, M., Pan, J., Bai, Y., and Liang, C.: Effects of typhoons on surface seawater pCO_2 and air-sea CO_2 fluxes in the northern South China Sea, J. Geophys. Res.-Oceans, 125, e2020JC016258, https://doi.org/10.1029/2020JC016258, 2020.

Yuan, X., He, L., Yin, K., Pan, G., and Harrison, P. J.: Bacterial distribution and nutrient limitation in relation to different water masses in the coastal and northwestern South China Sea in late summer, Cont. Shelf Res., 31, 1214–1223, 2011.

Zhang, C., Zhang, X., Zeng, Y., Pan, W., and Lin, J.: Retrieval and validation of sea surface temperature in the Taiwan Strait using MODIS data, Acta Oceanol. Sin., 30, 153–160, 2008.

Zhang, C., Ren, Y., Cai, Y., Zeng, Y., and Zhang, X.: Study on local monitoring model for SST in Taiwan strait based on MODIS data, J. Trop. Meteorol., 25, 73–81, 2009.

Zhong, Y. P., Liu, X., Xiao, W. P., Laws, E. A., Chen, J. X., Wang, L., Liu, S. G., Zhang, F., and Huang, B. Q.: Phytoplankton community patterns in the Taiwan Strait match the characteristics of their realized niches, Prog. Oceanogr., 186, 1–15, 2020.